Landau-Pomeranchuk-Migdal effect in QCD and radiative energy loss in a quark-gluon plasma

Xin-Nian Wang
Nuclear Science Division, Mailstop 70A-3307, Lawrence Berkeley Laboratory, University of California, Berkeley, California 94720

Miklos Gyulassy
Physics Department, Columbia University, New York, New York 10027

Michael Plümer
Nuclear Science Division, Mailstop 70A-3307, Lawrence Berkeley Laboratory, University of California, Berkeley, California 94720
*and Physics Department, University of Marburg, D-35032 Marburg, Germany**
(Received 23 August 1994)

The non-Abelian analogue of the Landau-Pomeranchuk-Migdal effect is investigated in perturbative QCD. Extending our previous studies, the suppression of induced soft bremsstrahlung due to multiple scatterings of quarks in the spinor representation is considered. The effective formation time of gluon radiation due to the color interference is shown to depend on the color representation of the emitting parton, and an improved formula for the radiative energy loss is derived that interpolates between the factorization and Bethe-Heitler limits.

PACS number(s): 24.85.+p, 12.38.Mh, 13.87.Ce, 25.75.+r

I. INTRODUCTION

Ultrarelativistic heavy ion collisions at future collider energies of the BNL Relativistic Heavy Ion Collider (RHIC) and CERN Large Hadron Collider (LHC) are expected to reveal novel QCD dynamics not accessible at present fixed target energies. When the transverse momentum transfer involved in each nucleon-nucleon collision is small, $p_T \lesssim \Lambda_{\rm QCD}$, effective models based on meson exchange and resonance formation are sufficient to describe multiple interactions between hadrons. Those interactions lead to collective behavior in low-energy heavy ion collisions as first observed in experiments [1] at the LBL collider Bevalac and recently at energies reached at the BNL Alternating Gradient Synchrotron (AGS) [2]. When p_T becomes large enough to resolve individual partons inside a nucleon, the dynamics is best described on the parton level via perturbative QCD. Though hard parton interactions occur at energies reached at the CERN Super Proton Synchrotron (SPS) ($E_{\rm lab} < 200A$ GeV), they play a negligible role in the global features of heavy ion collisions. However, at collider energies ($E_{\rm c.m.} > 100A$ GeV) the importance of hard or semihard parton scatterings is clearly seen in high-energy pp and $p\bar{p}$ collisions [3]. They are therefore also expected to be dominant in heavy ion collisions at RHIC and LHC energies [4,5].

Since hard parton scatterings occur very early (~ 0.01 fm/c) and their rates are calculable via perturbative QCD (PQCD), we proposed in [6,7] that high p_T parton jets could serve as a unique probe of the quark-gluon plasma formed due to copious minijet production over longer time scales (> 0.1 fm/c). The systematics of jet quenching provides information on the stopping power, dE/dz, of high-energy partons in dense matter [8]. The stopping power is in turn controlled by the color screening scale μ in the medium. Thus, jets provide information on that interesting dynamical scale in deconfined matter. At very high energy densities, that scale is expected to be large compared to the confinement scale [9]. At temperatures $T \gg T_c$, for example, we expect $\mu \sim gT \gg \Lambda_{\rm QCD}$. In that case, most partonic interactions have high momentum transfers and perturbative QCD methods may apply to the calculation of multiple collision amplitudes.

In Ref. [10] a systematic study of QCD multiple collision theory was initiated with the aim of deriving the non-Abelian analogue of the Landau-Pomeranchuk-Migdal (LPM) effect. That effect, first derived in the case of QED [11,12], involves destructive interference between bremsstrahlung radiation amplitudes. It suppresses radiation relative to the Bethe-Heitler formula in kinematic regions where the radiation formation time is long compared to the mean free path. In QCD a similar effect is also expected because it mainly follows from general relativistic uncertainty principle arguments. However, we showed in [10] that specific non-Abelian effects influence the detailed interference pattern in the case of QCD.

The LPM effect in QCD is especially important for estimating the energy loss dE/dz of an energetic parton traversing a dense QCD medium. We note that there exists considerable controversy in the literature on the magnitude and energy dependence of the energy loss in

*Permanent address.

QCD [13–17]. In this paper we extend our derivation in [10] to clarify further this effect and improve our previous estimates of dE/dz.

In the next section, we consider in detail the problem of induced gluon radiation from a spin-1/2 quark suffering two elastic scatterings. This provides insight into the applicability of the effective potential model used in Ref. [10] to calculate multiple collision amplitudes. We show why radiation from the target partons is negligible although such amplitudes are absolutely necessary to ensure gauge invariance. On the other hand, gauge invariance constrains all gluon propagators to be regulated by the same screening mass in the potential model. In Sec. III, the QCD radiation interference pattern is shown to be expressible as a function of an effective formation time that depends on the color representation of the jet parton. In Sec. IV, that formation time is used to calculate the average radiative energy loss dE/dz and derive a simple formula that interpolates between the factorization and Bethe-Heitler limits as a function of a dimensionless ratio depending on the incident parton energy E, the screening scale, and the mean free path. Finally, Sec. V contains a summary and closing remarks.

II. POTENTIAL MODEL AND GAUGE INVARIANCE

To analyze multiple parton scatterings and the induced gluon radiation, certain simplifications have to be made for the interaction. Consider the scattering of a high-energy jet parton in a color-neutral quark-gluon plasma. If the average distance $\Delta z = \lambda$ between two successive scatterings is large compared to the color screening length $\lambda \gg \mu^{-1}$, the effective average random color field produced by the target partons can be modeled by a static Debye screened potential:

$$V^a_{AA'}(\mathbf{q}) = A^a_{AA'}(\mathbf{q})e^{-i\mathbf{q}\cdot\mathbf{x}} = gT^a_{AA'}\frac{e^{-i\mathbf{q}\cdot\mathbf{x}}}{\mathbf{q}^2+\mu^2}, \tag{1}$$

where μ is the color screening mass and T^a are the generators of SU(3) corresponding to the representation of the target parton at $\mathbf{x}$. The initial and final color indices A, A' of the target parton are averaged and summed over when calculating the ensemble-averaged cross sections. This model potential was used in Ref. [10] to calculate cross sections of multiple scattering and induced radiation. However, to obtain a gauge-invariant amplitude of gluon radiation in QCD, every diagram with a fixed number of final gluon lines has to be taken into account, including gluon radiation from the target parton line. Radiation from target partons cannot be described by the above static model potential. The relative importance of different diagrams to the net energy loss depends on the choice of the gauge. In the light-cone gauge one expects radiation from target legs to be negligible as compared to that from the high-energy beam parton.

To estimate the importance of target radiation to the energy loss of a fast parton and to see how the gauge invariance constrains the potential model, consider the simplest case of induced radiation from quark-quark scatterings. The Born amplitude for $(p_i,k_i)\to(p_f,k_f)$ through one-gluon exchange is

$$\mathcal{M}_{\rm el} = ig^2T^a_{AA'}T^a_{BB'}\frac{\bar u(p_f)\gamma_\mu u(p_i)\bar u(k_f)\gamma^\mu u(k_i)}{(k_i-k_f)^2}, \tag{2}$$

where A, A', B, and B' are the initial and final color indices of the beam and target partons, respectively. The corresponding elastic cross section is

$$\frac{d\sigma_{\rm el}}{dt} = C^{(1)}_{\rm el}\frac{2\pi\alpha_s^2}{s^2}\frac{s^2+u^2}{t^2}, \tag{3}$$

where $C^{(1)}_{\rm el} = C_F/2N = 2/9$ is the color factor for a single elastic quark-quark scattering and s, u, and t are the Mandelstam variables.

For induced radiation, there are all together three groups of diagrams as shown in Fig. 1. If we rewrite the three amplitudes as

$$\mathcal{M}^{(i)}_{\rm rad} \equiv \widehat{\mathcal{M}}^{(i)}_\mu\epsilon^\mu, \tag{4}$$

then gauge invariance implies that

$$\sum_{i=1}^{3}\widehat{\mathcal{M}}^{(i)}_\mu k^\mu = 0, \tag{5}$$

where ϵ and k are, respectively, the polarization and momentum of the radiated gluon. In the soft radiation limit, we can neglect all the terms proportional to k_μ in $\widehat{\mathcal{M}}^{(i)}_\mu$ which does not contribute to $\widehat{\mathcal{M}}^{(i)}_\mu k^\mu(k^2=0)$. The complete and gauge-invariant amplitude for induced gluon radiation is

$$\begin{aligned}\mathcal{M}_{\rm rad} = ig^3\bar u(p_f)\gamma_\mu u(p_i)\bar u(k_f)\gamma^\mu u(k_f)\Bigg\{&\frac{1}{(k_i-k_f)^2}\left[\frac{\epsilon\cdot p_f}{k\cdot p_f}(T^bT^a)_{BB'}-\frac{\epsilon\cdot p_i}{k\cdot p_i}(T^aT^b)_{BB'}\right]T^a_{AA'}\\&+\frac{1}{(p_i-p_f)^2}\left[\frac{\epsilon\cdot k_f}{k\cdot k_f}(T^bT^a)_{AA'}-\frac{\epsilon\cdot k_i}{k\cdot k_i}(T^aT^b)_{AA'}\right]T^a_{BB'}\\&+\frac{1}{(p_i-p_f)^2(k_i-k_f)^2}[\epsilon\cdot(k_f-k_i)-\epsilon\cdot(p_f-p_i)]C^b_{AA',BB'}\Bigg\},\end{aligned} \tag{6}$$

where b is the color index of the radiated gluon and

$$C^b_{AA',BB'} = [T^a,T^b]_{BB'}T^a_{AA'} = -T^a_{BB'}[T^a,T^b]_{AA'} \tag{7}$$

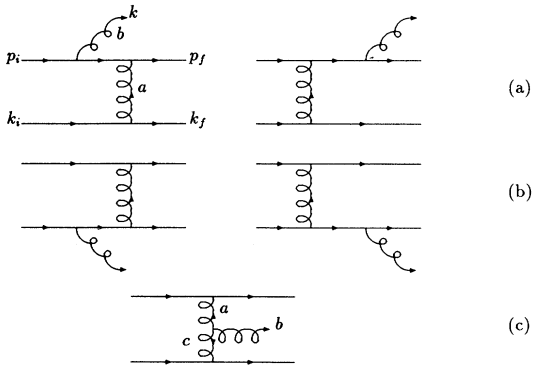

FIG. 1. Diagrams for induced gluon radiation from a single qq scattering.

are the color matrices associated with gluon radiation from the internal gluon line [Fig. 1(c)]. The three terms in Eq. (6) correspond to the radiation from the projectile [Fig. 1(a)], target parton [Fig. 1(b)], and the internal gluon line [Fig. 1(c)]. As one can see, no term alone is separately invariant under a gauge transformation $\epsilon^\mu \to \epsilon^\mu + c\,k^\mu$. Only the total amplitude is gauge invariant.

In the potential model, one simply neglects the radiation from the target lines and replaces the gluon-exchange amplitude associated with the target parton, $gT^a_{AA'}\bar{u}(k_f)\gamma^\mu u(k_i)/(k_i-k_f)^2$, by an effective potential $g^{\mu 0}A^a_{AA'}$. The potential given by Eq. (1) is regularized by the color screening mass squared μ^2. However, in Eq. (6), if any of the gluon propagators is regulated, gauge invariance is preserved only if all propagators are regulated with the same mass squared μ^2. In particular, the two propagators in the internal radiation diagram must both be regulated by the same scale.

While gauge invariance is manifest only if all diagrams are added, we now show that, in the $A^+ = 0$ gauge, only the projectile diagrams contribute significantly to the radiation of soft gluons in the dominant kinematic range for the net energy loss. We consider the case that a gluon with light-cone momentum and polarization,

$$k = [xP^+, k_\perp^2/xP^+, \mathbf{k}_\perp],$$
$$\epsilon = [0, 2\vec{\epsilon}_\perp\cdot\mathbf{k}_\perp/xP^+, \vec{\epsilon}_\perp], \tag{8}$$

is radiated off a high-energy quark with initial momentum

$$p_i = [P^+, 0, \mathbf{0}_\perp]. \tag{9}$$

During the interaction, the beam quark exchanges a momentum

$$q = [q^+, q^-, \mathbf{q}_\perp] \tag{10}$$

with a target quark which has a typical thermal momentum

$$k_i = [M, M, \mathbf{0}_\perp], \tag{11}$$

with $M \sim T$ in the plasma rest frame. We focus on the limit defined by $x \ll 1$, however, with the condition $xP^+ \gg M \gg q_\perp$. By requiring both of the final quarks to emerge on mass shell, one finds that

$$q^+ \simeq -\frac{q_\perp^2}{M},$$
$$q^- \simeq \frac{(\mathbf{q}_\perp-\mathbf{k}_\perp)^2}{(1-x)P^+} + \frac{k_\perp^2}{xP^+}. \tag{12}$$

The final momenta of the beam and target partons are, respectively,

$$p_f = p_i + q - k \simeq \left[(1-x)P^+, \frac{(\mathbf{q}_\perp-\mathbf{k}_\perp)^2}{(1-x)P^+}, \mathbf{q}_\perp-\mathbf{k}_\perp\right],$$
$$k_f = k_i - q \simeq [M + q_\perp^2/M, M, -\mathbf{q}_\perp]. \tag{13}$$

With the above kinematics, one can obtain the momentum elements of the radiation amplitudes:

$$\frac{\epsilon\cdot p_f}{k\cdot p_f} \simeq \frac{\epsilon\cdot p_i}{k\cdot p_i} = 2\frac{\vec{\epsilon}_\perp\cdot\mathbf{k}_\perp}{k_\perp^2}, \tag{14}$$

$$\frac{\epsilon\cdot k_i}{k\cdot k_i} \simeq 2\frac{\vec{\epsilon}_\perp\cdot\mathbf{k}_\perp}{(xP^+)^2} \quad \frac{\epsilon\cdot k_f}{k\cdot k_f} \simeq 2\frac{\vec{\epsilon}_\perp\cdot\mathbf{q}_\perp}{xP^+M}. \tag{15}$$

In the large $xP^+ \gg k_\perp$ limit, we see that the magnitudes of the matrix elements involving target parton radiation in Eq. (15) are much smaller than those involving projectile radiation in Eq. (14). As we will see below, the LPM effect limits the radiation to $x < \lambda\mu^2/P^+$ and $k_\perp < \mu$. Therefore, as long as $\lambda\mu \gg 1$, the contribution to the energy loss in the main kinematic range is dominated by the projectile radiation in this gauge. However, as we have demonstrated, the small target contributions to the radiation amplitude are amplified if ϵ^μ is replaced by k^μ. As a result of this amplification, those amplitudes cannot be neglected when considering gauge invariance even though they can be neglected for calculating the energy loss.

Taking into account only the dominant contributions to the radiation amplitude, we have the factorized amplitude

$$\mathcal{M}_{\rm rad} \equiv \frac{\mathcal{M}_{\rm el}}{T^a_{AA'}T^a_{BB'}} i\mathcal{R}_1,$$
$$\mathcal{R}_1 \simeq 2ig\vec{\epsilon}_\perp\cdot\left[\frac{\mathbf{k}_\perp}{k_\perp^2} + \frac{\mathbf{q}_\perp-\mathbf{k}_\perp}{(\mathbf{q}_\perp-\mathbf{k}_\perp)^2}\right] T^a_{AA'}[T^a, T^b]_{BB'}, \tag{16}$$

where $\mathcal{M}_{\rm el}$ is the elastic amplitude as given in Eq. (2) and $\mathcal{R}_1$ is defined as the radiation amplitude induced by a single scattering. For later convenience, all the color matrix elements are included in the definition of the radiation amplitude $\mathcal{R}_1$. With the above approximations, we recover the differential cross section for induced gluon bremsstrahlung by a single collision as originally derived by Gunion and Bertsch [18],

$$\frac{d\sigma}{dtdyd^2k_\perp} = \frac{d\sigma_{\rm el}}{dt}\frac{dn^{(1)}}{dyd^2k_\perp}, \tag{17}$$

where the spectrum for the radiated gluon is

$$\frac{dn^{(1)}}{dyd^2k_\perp} \equiv \frac{1}{2(2\pi)^3 C_{\rm el}^{(1)}} \overline{|\mathcal{R}_1|^2} = \frac{C_A\alpha_s}{\pi^2} \frac{q_\perp^2}{k_\perp^2(\mathbf{q}_\perp - \mathbf{k}_\perp)^2}. \tag{18}$$

In the square modulus of the radiation amplitude, an average and a sum over initial and final color indices and polarization are understood. We see that the spectrum has a uniform distribution in central rapidity region (small x) which is a well-known feature of QCD soft radiation [19]. This feature is consistent with the hadron distributions predicted by Lund string models and the "string effects" in e^+e^- three jets events [20,21], all being the results of interference effects of PQCD radiation. To demonstrate this a little in detail, let us consider only the radiation amplitude from the beam quark in Eq. (6):

$$\mathcal{R} = \left[\frac{\epsilon\cdot p_f}{k\cdot p_f}(T^bT^a)_{BB'} - \frac{\epsilon\cdot p_i}{k\cdot p_i}(T^aT^b)_{BB'}\right] T^a_{AA'}. \tag{19}$$

The corresponding gluon spectrum is [in addition to a factor $1/2(2\pi)^3$]

$$\frac{1}{C_{\rm el}^{(1)}}\overline{|\mathcal{R}|^2} = C_F\left[\frac{\epsilon\cdot p_i}{k\cdot p_i} - \frac{\epsilon\cdot p_f}{k\cdot p_f}\right]^2 + \frac{C_A}{2}2\frac{\epsilon\cdot p_i}{k\cdot p_i}\frac{\epsilon\cdot p_f}{k\cdot p_f}, \tag{20}$$

where $C_F = (N^2-1)/2N$ and $C_A = N$ are the second-order Casimir invariants for quarks in the fundamental and for gluons in the adjoint representation, respectively. Note that the first term is identical to gluon radiation induced by an Abelian gauge interaction like a photon exchange and does not contribute to the gluon spectrum in the central rapidity region due to the destructive interference of the initial and final state radiations. The second term arises from the non-Abelian interactions with the target partons and is the main contribution to the central region.

Another non-Abelian feature in the induced gluon radiation amplitude, Eq. (16), is the singularity at $\mathbf{k}_\perp = \mathbf{q}_\perp$ due to induced radiation along the direction of the exchanged gluon. For $k_\perp \ll q_\perp$, we note that the induced radiation from a three-gluon vertex can be neglected as compared to the leading contribution $1/k_\perp^2$. However, at large $k_\perp \gg q_\perp$, this three-gluon amplitude is important to change the gluon spectrum to a $1/k_\perp^4$ behavior, leading to a finite average transverse momentum. Therefore, $q_\perp$ may serve as a cutoff for $k_\perp$ when one neglects the amplitude with the three-gluon vertices as we will do when we consider induced radiation by multiple scatterings in the next section. If one wishes to include the three-gluon amplitude, then the singularity at $\mathbf{k}_\perp = \mathbf{q}_\perp$ has to be regularized. As we have discussed above, the regularization scheme has to be the same as for the model potential or the gluon propagator in $d\sigma_{\rm el}/dt$ as required by gauge invariance. In our case, a color screening mass μ will be used.

III. EFFECTIVE FORMATION TIME

The radiation amplitude induced by multiple scatterings has been discussed in Ref. [10]. We discuss here the special case of double scatterings to gain further insight into the problem. Consider two static potentials separated by a distance L, which is assumed to be much larger than the interaction length $1/\mu$. In the Abelian case, the radiation amplitude associated with double scatterings is (see the Appendix)

$$\mathcal{R}_2^{\rm QED} = ig\left[\left(\frac{\epsilon\cdot p_i}{k\cdot p_i} - \frac{\epsilon\cdot p}{k\cdot p}\right)e^{ik\cdot x_1} + \left(\frac{\epsilon\cdot p}{k\cdot p} - \frac{\epsilon\cdot p_f}{k\cdot p_f}\right)e^{ik\cdot x_2}\right], \tag{21}$$

where $p = (p_f^0, p_z, \mathbf{p}_\perp)$ is the four-momentum of the intermediate parton line which is put on mass shell by the pole in one of the parton propagators, $x_1 = (0, \mathbf{x}_1)$, and $x_2 = (t_2, \mathbf{x}_2)$ are the four-coordinates of the two potentials with $t_2 = (z_2 - z_1)/v_z = Lp^0/p_z$. This formula has been recently used to discuss interference effects on photon and dilepton production in a quark-gluon plasma [22,23]. We notice that the amplitude has two distinct contributions from each scattering. Especially, the diagram [Fig. 2(b)] with a gluon radiated from the intermediate line between the two scatterings contributes both as the final state radiation for the first scattering and the initial state radiation for the second scattering. The relative phase factor

$$k\cdot(x_2 - x_1) = \omega(1/v_z - \cos\theta)L \equiv L/\tau(k)$$

determines the interference between radiations from the two scatterings and is simply the ratio of the path length to the formation time defined as

$$\tau(k) = \frac{1}{\omega(1/v_z - \cos\theta)} \simeq \frac{2\omega}{k_\perp^2}. \tag{22}$$

The Bethe-Heitler limit is reached when $L \gg \tau(k)$. In this limit, the intensity of induced radiation is additive in the number of scatterings. However, when $L \ll \tau(k)$, the final state radiation amplitude from the first scattering is mostly canceled by the initial state radiation amplitude from the second scattering. The radiation pattern then looks as if the parton has only suffered a single scattering from p_i to p_f. This destructive interference is often referred to as the Landau-Pomeranchuk-Migdal (LPM) effect. The corresponding limit is usually called the factorization limit.

The radiation amplitude in QCD is similar to Eq. (21), except that one has to include different color factors for each diagram in Fig. 2. In the high-energy limit, $\epsilon\cdot p_i/k\cdot p_i \simeq \epsilon\cdot p/k\cdot p \simeq \epsilon\cdot p_f/k\cdot p_f \simeq 2\vec{\epsilon}_\perp\cdot\mathbf{k}_\perp/k_\perp^2$. The momentum dependence of each contribution can be factored out and

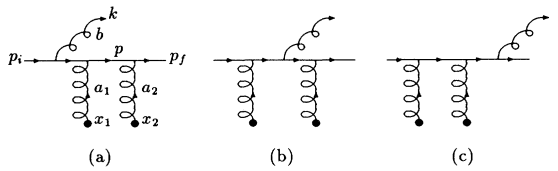

FIG. 2. Diagrams for gluon radiation from the quark line induced by double scatterings.

the radiation amplitude for diagrams in Fig. 2 is

$$\mathcal{R}_2 = i2g\frac{\vec{\epsilon}_\perp\cdot\mathbf{k}_\perp}{k_\perp^2}\Big\{\left(T^{a_2}[T^{a_1},T^b]\right)_{BB'}e^{ik\cdot x_1} + \left([T^{a_2},T^b]T^{a_1}\right)_{BB'}e^{ik\cdot x_2}\Big\}T^{a_1}_{A_1A_1'}T^{a_2}_{A_2A_2'}, \quad (23)$$

where we have included two color matrices from the potentials and b again represents the color index of the radiated gluon. The radiation amplitude from diagrams with three-gluon vertices has the same phase and color structures as in Eq. (23), but the momentum dependence cannot be factorized, since each term depends on the transverse momentum transfer which differs from one scattering to another. However, since we are interested in the soft radiation limit $k_\perp < q_\perp \sim \mu$, the contributions from internal gluon line emissions can be neglected as shown in [10]. As we discussed above, however, those amplitudes serve to provide an effective cutoff $\langle q_\perp\rangle \sim \mu$ for $k_\perp$.

The extrapolation of Eq. (23) to the general case of m number of scatterings is straightforward with the result

$$\mathcal{R}_m = i2g\frac{\vec{\epsilon}\cdot\mathbf{k}_\perp}{k_\perp^2}T^{a_1}_{A_1A_1'}\cdots T^{a_m}_{A_mA_m'} \times\sum_{i=1}^{m}\left(T^{a_m}\cdots[T^{a_i},T^b]\cdots T^{a_1}\right)_{BB'}e^{ik\cdot x_i}. \quad (24)$$

The above amplitude contains m terms, each having a common momentum dependence in the high-energy limit, but with different color and phase factors. The above expression is also valid for a gluon beam jet, with the corresponding color matrices replaced by those of an adjoint representation. In Eq. (24), we also assumed that all potentials have a color structure of a fundmental representation. One can generalize to the case in which each individual potential could have any arbitrary color representation. However, our following results on the gluon spectrum and interference pattern will remain the same. With this in mind, we have the spectrum of soft bremsstrahlung associated with multiple scatterings in a color-neutral ensemble, similar to Eq. (18),

$$\frac{dn^{(m)}}{dyd^2k_\perp} = \frac{1}{2(2\pi)^2C_{\rm el}^{(m)}}\overline{|\mathcal{R}_m|^2} \equiv C_m(k)\frac{dn^{(1)}}{dyd^2k_\perp}, \quad (25)$$

where $C_{\rm el}^{(m)} = (C_F/2N)^m$ is the color factor for the elastic scattering cross section without radiation. $C_m(k)$, defined as the "radiation formation factor" to characterize the interference pattern due to multiple scatterings, can be expressed as

$$C_m(k) = \frac{1}{C_F^mC_AN}\sum_{i=1}^{m}\left[C_{ii} + 2\,\mathrm{Re}\sum_{j=1}^{i-1}C_{ij}e^{ik\cdot(x_i-x_j)}\right], \quad (26)$$

where the color coefficients, as computed in Ref. [10], are

$$C_{ii} = C_F^mC_AN;$$
$$C_{ij} = -\frac{C_A}{2}\frac{C_A}{2C_F}\left(1-\frac{C_A}{2C_F}\right)^{i-j-1}C_F^mC_AN \quad \text{for } j<i. \quad (27)$$

For a gluon beam jet, one can simply change the dimension to that of an SU(N) adjoint representation and replace $C_2 = C_F$ by the corresponding second-order Casimir invariant $C_2 = C_A$. We then obtain a general form for the radiation formation factor for a high-energy parton jet:

$$C_m(k) = m - r_2\mathrm{Re}\sum_{i=1}^{m}\sum_{j=1}^{i-1}(1-r_2)^{i-j-1}e^{ik\cdot(x_i-x_j)}, \quad (28)$$

where

$$r_2 = \frac{C_A}{2C_2} = \begin{cases} N^2/(N^2-1) & \text{for quarks with } C_2 = C_F,\\ 1/2 & \text{for gluons with } C_2 = C_A.\end{cases} \quad (29)$$

Similar to the special case of double scatterings, there are a few interesting limits for the above general form of the radiation formation factor and the induced gluon spectrum. When $m = 1$, $C_1(k) = 1$. We recover the gluon spectrum induced by a single scattering in Eq. (18) in the small $k_\perp$ limit. For multiple scatterings in the Bethe-Heitler limit when $L_{ij} = |z_i - z_j| \gg \tau(k)$ for all $i > j$, the phase factors average to zero and the intensity of the radiation is additive in the number of scatterings, i.e., $C_m(k) \approx m$. In the factorization limit, one has $L_{ij} \ll \tau(k)$ for all $i > j$. In this case, the phase factors can be set to unity and the summations in Eq. (28) can be carried out to give

$$C_m(k) \approx \frac{1}{r_2}[1-(1-r_2)^m] = \begin{cases}\frac{8}{9}[1-(-1/8)^m] & \text{for quarks,}\\ 2(1-1/2^m) & \text{for gluons.}\end{cases} \quad (30)$$

In contrast with the Bethe-Heitler limit, the factorization limit is independent of the number of collisions as $m\to\infty$, and the radiation formation factor approaches $1/r_2 = 2C_2/C_A$. It is interesting to note that the destructive interference for quarks in the fundamental representation is so effective that the radiation spectrum induced by many scatterings is even slightly less, $1/r_2 = 8/9$, than by a single scattering. For gluon jets, however, the interference is not as complete as for quarks. The induced radiation approaches 2 times that from a single scattering. Using these values of $C_m(k) = 1/r_2 = 2C_2/C_A$ in Eqs. (25) and (18), the radiation intensity induced by multiple scatterings is proportional to $2C_2$ as compared to C_A in the single scattering case. The gluon intensity radiated by a gluon jet is therefore 9/4 higher than that by a quark due to the interference in multiple scatterings. This dependence of the LPM effect in QCD on the color representation of the beam parton is a unique non-Abelian effect. As we will discuss in the following, the effective formation time of the radiation in a QCD

medium should also take this non-Abelian effect into account.

To see analytically how $C_m(k)$ interpolates between the Bethe-Heitler and factorization limits, let us average over the interaction points $\mathbf{x}_i$ according to a linear kinetic theory. We take an eikonal approximation [10] for the multiple scatterings so that the transverse phase factors can be neglected in the soft radiation limit $k_\perp \ll q_\perp \sim \mu$. In a linear kinetic theory, the longitudinal separation between successive scatterings, $L_i = z_{i+1} - z_i$, has a distribution

$$\frac{dP}{dL_i} = \frac{1}{\lambda} e^{-L_i/\lambda}, \tag{31}$$

which is controlled by the mean free path λ of the scatterings. The averaging of the phase factors,

$$\langle e^{i\mathbf{k}\cdot(\mathbf{x}_i - \mathbf{x}_j)} \rangle \approx \left[\frac{1}{1 - i\lambda/\tau(k)} \right]^{i-j}, \tag{32}$$

enables us to complete the summation in Eq. (28). Neglecting terms proportional to $(1 - r_2)^m$ for relatively large m, we have

$$C_m(k) \approx m \frac{\chi^2(k)}{1 + \chi^2(k)} + \frac{1 - (1 - 2r_2)\chi^2(k)}{r_2[1 + \chi^2(k)]^2}. \tag{33}$$

The non-Abelian LPM effect in QCD is therefore controlled by the dimensionless ratio of the mean free path to an effective formation time,

$$\chi(k) = \lambda/\tau_{\rm QCD}(k), \tag{34}$$

where the effective formation time in QCD depends on the color representation of the jet parton and is related to the usual Abelian formation time in Eq. (22) as

$$\tau_{\rm QCD}(k) = r_2 \tau(k) = \frac{C_A}{2C_2} \frac{2\cosh y}{k_\perp}. \tag{35}$$

This formula for the radiation formation factor is illustrated in Fig. 3 as a function of $\tau(k)/\lambda$ for the case of five collisions ($m = 5$) and shows how $C_m(k)$ interpolates between the Bethe-Heitler limit for a small value of $\tau(k)/\lambda$ and the factorization limit for a large value of $\tau(k)/\lambda$. For radiation with average transverse momentum $k_\perp \sim \mu$ the additive Bethe-Heitler region is limited to rapidities $y < \ln(r_2 \lambda \mu)$. In general, the radiation formation factor is proportional to m in the limit of large m. We can therefore regard the radiation as being additive to the number of scatterings with the radiation from each scattering simply suppressed by the factor $\chi^2/(1 + \chi^2)$ due to the non-Abelian LPM effect. Since this effective formation time is a result of the unique color interference effect in QCD, we should use it in the following to estimate the radiative energy loss by a high-energy parton traversing a color-neutral quark-gluon plasma.

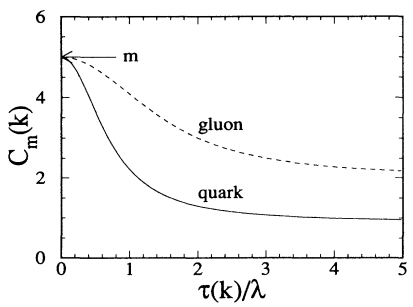

FIG. 3. The radiation formation factor $C_m(k)$, $m = 5$, as a function of $\tau(k)/\lambda = 2\cosh(y)/k_\perp\lambda$ for quarks (solid line) and gluons (dashed line).

IV. RADIATIVE ENERGY LOSS

We now apply the effective formation time to derive a simple approximate formula for the induced radiative energy loss extending our previous result in [10]. As shown in the previous section the radiation spectrum is given by Eq. (18) multiplied by the radiation formation factor Eq. (33). That factor simply restricts the additive kinematic region to $\tau_{\rm QCD}(k)/\lambda < 1$ and the the incremental change in that factor for each successive collision can be approximated by a pocket formula $dC_m(k)/dm \approx \theta(\lambda - \tau_{\rm QCD}(k))$ (see Fig. 3). The additive radiative energy loss for each collision beyond the first one is then

$$\begin{aligned} \Delta E_{\rm rad} \approx \int d^2k_\perp dy \frac{dn_g}{d^2k_\perp dy} k_\perp \\ \times \cosh y \, \theta(\lambda - \tau_{\rm QCD}(k)) \\ \times \theta(E - k_\perp \cosh y), \end{aligned} \tag{36}$$

where $\tau_{\rm QCD}(k)$ is given by Eq. (35), the second θ function is for energy conservation, and the regularized gluon density distribution induced by a single scattering is

$$\frac{dn_g}{d^2k_\perp dy} = \frac{C_A \alpha_s}{\pi^2} \frac{q_\perp^2}{k_\perp^2[(\mathbf{q}_\perp - \mathbf{k}_\perp)^2 + \mu^2]}. \tag{37}$$

As discussed earlier, gauge invariance requires that the singularity at $\mathbf{k}_\perp = \mathbf{q}_\perp$ in Eq. (18) must be regularized by the same color screening mass μ as in the elastic cross section in the potential model. Since the transverse momentum transfer $q_\perp$ is the result of elastic scatterings, we have to average any function $f(\mathbf{q}_\perp)$ of $\mathbf{q}_\perp$ by the elastic cross section:

$$\langle f(\mathbf{q}_\perp) \rangle = \frac{1}{\sigma_i} \int_{\mu^2}^{s/4} dq_\perp^2 \frac{d\sigma_i}{dq_\perp^2} f(\mathbf{q}_\perp), \tag{38}$$

where $s \approx 6ET$ is the average c.m. energy squared for the scattering of a jet parton with energy E off the thermal partons at temperature T. For the dominant small angle scattering, the elastic cross sections are

$$\frac{d\sigma_i}{dq_\perp^2} \cong C_i \frac{2\pi\alpha_s^2}{q_\perp^4}, \tag{39}$$

where $C_i = 9/4$, 1, and $4/9$, respectively, for gg, gq, and qq scatterings. This average can be approximated

by replacing $q_\perp^2$ in the numerator of Eq. (37) with its average value:

$$\langle q_\perp^2 \rangle = \mu^2 \ln \frac{3ET}{2\mu^2}. \tag{40}$$

In the denominator, we simply replace $\mathbf{q}_\perp^2$ by μ^2 after the angular integration. The remaining integration in Eq. (36) over the restricted phase space approximately leads to the simple analytic formula

$$\Delta E_{\rm rad} \approx \frac{C_A \alpha_s}{\pi} \langle q_\perp^2 \rangle \left(\frac{\lambda}{2r_2} I_1 + \frac{E}{2\mu^2} I_2 \right), \tag{41}$$

$$I_1 = \ln \left[\frac{r_2 E}{\mu^2 \lambda} + \sqrt{1 + \left(\frac{r_2 E}{\mu^2 \lambda} \right)^2} \right] - \ln \left[2 \left(\frac{r_2}{\mu \lambda} \right)^2 + \sqrt{1 + 4 \left(\frac{r_2}{\mu \lambda} \right)^4} \right], \tag{42}$$

$$I_2 = \ln \left[\frac{\mu^2 \lambda}{r_2 E} + \sqrt{1 + \left(\frac{\mu^2 \lambda}{r_2 E} \right)^2} \right] - \ln \left[\frac{2\mu^2}{E^2} + \sqrt{1 + \left(\frac{2\mu^2}{E^2} \right)^2} \right]. \tag{43}$$

In the small $k_\perp$ regime, the phase space is mainly restricted by a small effective formation time $\tau_{\rm QCD} < \lambda$, which gives the first term proportional to λ. For large $k_\perp$, the radiation becomes additive in a restricted phase space constrained by energy conservation. That region contributes to the second term which appears to be proportional to the incident energy E. However, in the high-energy limit the function $I_2 \propto 1/E$ and hence the radiated energy loss grows only as $\ln^2 E$.

The above derivation assumed that the mean free path is much larger than the interaction range specified by $1/\mu$. As we shall discuss below, this is satisfied in a quark-gluon plasma at least in the weak coupling limit. Therefore, we can neglect the second term in I_1. For a high-energy jet parton, $E \gg \mu$, we can also neglect the second term in I_2. The resulting radiative energy loss reduces in that case to the simple form

$$\frac{dE_{\rm rad}}{dz} = \frac{\Delta E_{\rm rad}}{\lambda} \approx \frac{C_2 \alpha_s}{\pi} \langle q_\perp^2 \rangle \left[\ln \left(\xi + \sqrt{1+\xi^2} \right) + \xi \ln \left(\frac{1}{\xi} + \sqrt{1 + \frac{1}{\xi^2}} \right) \right], \tag{44}$$

which depends on a dimensionless variable

$$\xi = \frac{r_2 E}{\mu^2 \lambda}. \tag{45}$$

Since we have used the gluon spectrum from a single scattering in Eq. (18) which is valid for all values of $k_\perp$, the full integration over $k_\perp$ results in the logarithmic energy dependence of $dE_{\rm rad}/dz$. This logarithmic dependence was absent in our derivation in Ref. [10] since there only the contribution from the very soft $k_\perp < \mu$ region was considered.

We see that the radiative energy loss $dE_{\rm rad}/dz$ thus obtained interpolates between the factorization and Bethe-Heitler limits as a function of the dimensionless ratio ξ. In the factorization limit, we fix $\mu\lambda \gg 1$ and let $E \to \infty$, so that $\xi \gg 1$. In this case, we can neglect the second term in Eq. (44) and have

$$\frac{dE_{\rm rad}}{dz} \approx \frac{C_2 \alpha_s}{\pi} \langle q_\perp^2 \rangle \ln \left(\frac{2r_2 E}{\mu^2 \lambda} \right), \quad \xi \gg 1. \tag{46}$$

Thus, the radiative energy loss in the factorization limit has only a logarithmic energy dependence (in addition to the energy dependence of $\langle q_\perp^2 \rangle$). Because of the non-Abelian nature of the color interference, the resultant energy loss for a gluon ($C_2 = C_A$) is 9/4 times larger than that for a quark ($C_2 = C_F$). In the other extreme limit, we fix E and let $\mu\lambda \to \infty$, so that $\xi \ll 1$. In this case, the mean free path exceeds the effective formation time. The radiation from each scattering adds up. We then recover the linear dependence of the energy loss $dE_{\rm rad}/dz$ on the incident energy E (modulo logarithms):

$$\frac{dE_{\rm rad}}{dz} \approx \frac{C_A \alpha_s}{2\pi\lambda} \frac{\langle q_\perp^2 \rangle}{\mu^2} E \ln \left(\frac{2\mu^2 \lambda}{r_2 E} \right), \quad \xi \ll 1, \tag{47}$$

as in the Bethe-Heitler formula. In both cases, the radiative energy loss is proportional to the average of the transverse momentum transfer, $\langle q_\perp^2 \rangle$, which is controlled by the color screening mass as in Eq. (40).

To see more clearly how the factorization limit is approached, we now estimate ξ for a parton propagating inside a high-temperature quark-gluon plasma. From Eq. (39) and the perturbative QCD expressions for the quark and gluon densities at temperature T the mean free path for three quark flavors is

$$\lambda_q^{-1} = \sigma_{qq}\rho_q + \sigma_{qg}\rho_g \approx \frac{2\pi\alpha_s^2}{\mu^2} 4 \times 7\zeta(3) \frac{T^3}{\pi^2}, \tag{48}$$

$$\lambda_g^{-1} = \sigma_{qg}\rho_q + \sigma_{gg}\rho_g \approx \frac{2\pi\alpha_s^2}{\mu^2} 9 \times 7\zeta(3) \frac{T^3}{\pi^2}, \tag{49}$$

where $\zeta(3) \approx 1.2$. We emphasize that the above mean free path corresponds approximately to the color relaxation mean free path λ_c, and not the momentum relaxation mean free path λ_p. As shown in Ref. [24], $\lambda_c \sim \alpha_s \lambda_p$ is generally the shorter of the two in QCD. The reason why the color relaxation mean free path controls the radiation pattern is that the color current responsible for emitting the gluons is coherent only over a distance scale λ_c. It takes a much longer path length to stop a parton. However, unlike in QED, this longer momentum relaxation mean free path is irrelevant for non-Abelian radiation.

Using Eqs. (48) and (49) and the perturbative color electric screening mass $\mu^2 = 4\pi\alpha_s T^2$, we see that ξ appearing in the logarithms has a common energy and temperature dependence for both quarks and gluons:

$$\xi = \frac{r_2 E}{\lambda \mu^2} = \frac{63\zeta(3)}{16\pi^3}\frac{E}{T} \approx \frac{9}{2\pi^3}\frac{E}{T} \quad \text{for both } q \text{ and } g. \quad (50)$$

With the above expression for ξ, we plot the radiative energy loss in Fig. 4 as a function of the beam energy inside a plasma at temperature $T = 300$ MeV with $\alpha_s = 0.3$. The solid line is the full expression in Eq. (44) while the dashed line is the factorization limit corresponding to the first term in Eq. (44). We see that Eq. (46) approximates Eq. (44) quite well in this parameter range. The energy dependence of the radiative energy loss is due to the double logarithmic function in the formula, one of which comes from the energy dependence of the average transverse momentum $\langle q_\perp^2 \rangle$ in Eq. (40).

The energy loss of a quark in dense matter due to elastic scattering was first estimated by Bjorken [25] and later was studied in detail [26] in terms of finite-temperature QCD. For our purpose, a simple estimate taking into account both the thermal average and color screening will suffice. In terms of elastic cross sections and the density distributions for quarks and gluons in a plasma, we have

$$\frac{dE_{\rm el}}{dz} = \int_{\mu^2}^{s/4} dq_\perp^2 \frac{d\sigma_i}{dq_\perp^2}\rho_i \nu = \langle q_\perp^2 \rangle \sigma_i \left\langle \frac{\rho_i}{2\omega} \right\rangle, \quad (51)$$

where $\nu \approx q_\perp^2/2\omega$ is the energy transfer of the jet parton to a thermal parton with energy ω during an elastic scattering and $\langle q_\perp^2 \rangle$ is the average transverse momentum transfer given by Eq. (40). Similar to Eqs. (48) and (49), we have

$$\sigma_{qq}\left\langle \frac{\rho_q}{2\omega} \right\rangle + \sigma_{qg}\left\langle \frac{\rho_g}{2\omega} \right\rangle = \frac{2\pi\alpha_s^2}{\mu^2}T^2, \quad (52)$$

$$\sigma_{gq}\left\langle \frac{\rho_q}{2\omega} \right\rangle + \sigma_{gg}\left\langle \frac{\rho_g}{2\omega} \right\rangle = \frac{9}{4}\frac{2\pi\alpha_s^2}{\mu^2}T^2. \quad (53)$$

The elastic energy loss of a fast parton inside a quark-gluon plasma at temperature T is then given by

$$\frac{dE_{\rm el}}{dz} = C_2 \frac{3\pi\alpha_s^2}{2\mu^2}T^2\langle q_\perp^2 \rangle. \quad (54)$$

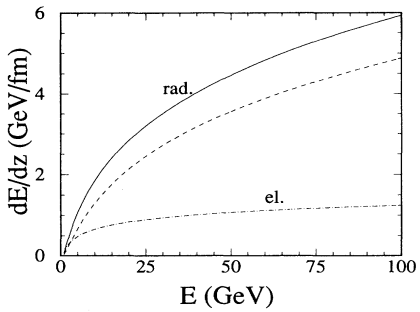

FIG. 4. The energy dependence of energy loss dE/dz of a quark with energy E inside a quark-gluon plasma at temperature $T = 300$ MeV. A weak coupling $\alpha_s = 0.3$ is used. The solid line is the full expression and the dashed line is the factorization limit of the radiative energy loss. The dot-dashed line is the elastic energy loss.

For comparison, we plot this elastic energy loss in Fig. 4. In general, it is much smaller than the radiative energy loss and has a weaker energy dependence (single logarithmic).

Using Eqs. (40), (46), and (50), the total energy loss can be expressed as

$$\frac{dE}{dz} = \frac{dE_{\rm el}}{dz} + \frac{dE_{\rm rad}}{dz} \approx \frac{C_2\alpha_s}{\pi}\mu^2 \ln\frac{3ET}{2\mu^2}\left(\ln\frac{9E}{\pi^3 T} + \frac{3\pi^2\alpha_s}{2\mu^2}T^2\right). \quad (55)$$

It is interesting to note that both the elastic and radiative energy losses have the same color coefficient C_2. For high-energy partons, the radiative energy loss is dominant over the elastic one. For $E = 30$ GeV, $T = 300$ MeV, and $\alpha_s \approx 0.3$, the total energy loss for a propagating quark is $dE/dz \approx 3.6$ GeV/fm. Only about 25% of this amount comes from elastic energy loss.

V. SUMMARY AND DISCUSSION

We extended our previous derivation by considering the role of gauge invariance and target radiation in the case of spin-1/2 quarks to improve our estimate of radiative energy loss of a fast parton inside a quark-gluon plasma. Our main result [Eq. (44)] interpolates between the factorization and Bethe-Heitler limits, and has unique non-Abelian properties. The factorization limit is of course consistent with the general bound [16] imposed by the uncertainty principle, but reveals a peculiar energy and temperature dependence of the mean square radiation transverse momentum controlling that energy loss. The total energy loss is very sensitive to the color screening scale in the plasma. The double logarithmic energy dependence of $dE_{\rm rad}/dz$ is the result of non-Abelian aspects of the LPM effect in QCD. The same effect should be responsible for the limited gluon equilibration rate as discussed in Ref. [27].

Our derivation improves that in [8,10] in a number of ways. First, an effective formation time $\tau_{\rm QCD}$ in QCD radiation was used to account for the color interference due to multiple scatterings. The dependence of this effective formation time on the color representation of the jet parton gave rise to the different color factors, proportional to C_2, for the radiative energy loss of a quark and gluon. In contrast both are proportional to C_A in the case of a single scattering. Second, the gluon spectrum including radiation from both the jet line and the internal gluon line and regulated consistently with the requirement of gauge invariance was used. However, Eq. (44) is still an idealization to the physically realizable situation in nuclear collisions because a number of strong assumptions were made in its derivation. The strongest is the extrapolation of PQCD in a regime $g \sim 1$ and the assumption that the interaction range is small compared to the color relaxation mean free path. We are therefore left with an explicit dependence on μ in dE/dz since strong nonperturbative variations of $\mu(T)$ occur in the vicinity of T_c. The basic result that dE/dz is propor-

tional to μ^2 is, however, very general and consistent with the uncertainty bounds in [16]. Therefore, in a separate paper [28], we will investigate the phenomenological consequences of the interesting temperature dependence of $\mu(T)$ suggested by lattice calculations.

ACKNOWLEDGMENTS

We would like to thank J. Cleymans, J. Knoll, and B. Müller for stimulating discussions. This work was supported by the Director, Office of Energy Research, Division of Nuclear Physics of the Office of High Energy and Nuclear Physics of the U.S. Department of Energy under Contract No. DE-AC03-76SF00098 and DE-FG02-93ER40764.

APPENDIX

The radiation amplitude within multiple scattering theory has been derived in Ref. [10] in a general from. In this appendix we use the radiation induced by double scattering as an example to demonstrate how the general formula arises from the multiple scattering theory. We consider the scattering of a high-energy particle off potentials as given by Eq. (1). For simplicity, let us first neglect the color indices as in the case of QED. The amplitude for a single scattering is then

$$\mathcal{M}^{(1)}_{\rm el} = 2\pi i\delta(E_i - E_f)4\pi E f_1(E,t), \tag{A1}$$

$$f_1(E,t) = \frac{-i}{2\pi}\frac{g}{2Ei}\bar{u}_{\sigma_f}(p_f)\,\not{A}(\mathbf{q})u_{\sigma_i}(p_i)e^{-i\mathbf{q}\cdot\mathbf{x}}, \tag{A2}$$

where $E = E_i = E_f$ and the amplitude $f(E,t)$ is defined such that the differential cross section is given by

$$\frac{d\sigma}{dt} = \pi|f(E,t)|^2, \tag{A3}$$

and σ_i, σ_f are the initial and final polarizations which should be averaged and summed over in the calculation of cross sections. One can check that with the definition of $A(\mathbf{q})$ in Eq. (1), the above formula leads to $d\sigma/dt = 4\pi\alpha_s^2/(\mathbf{q}^2+\mu^2)^2$.

One can similarly write down the amplitude for double scatterings,

$$\mathcal{M}^{(2)}_{\rm el} = 2\pi i\delta(E_i - E_f)(-g^2)\int\frac{d^3\ell}{(2\pi)^3}\bar{u}_{\sigma_f}(p_f)\,\not{A}(\mathbf{p}_f-\ell) \times\frac{\not{\ell}}{\ell^2+i\epsilon}\,\not{A}(\ell-\mathbf{p}_i)u_{\sigma_i}(p_i)e^{-i(\ell-\mathbf{p}_i)\cdot\mathbf{x}_1 - i(\mathbf{p}_f-\ell)\cdot\mathbf{x}_2}, \tag{A4}$$

where the energy conservation at each potential vertex sets the energy of the internal line to $\ell^0 = E = E_f$. Amplitudes involving backscattering are suppressed at high energies because of the limited momentum transfer that each potential can impart. When the mean free path (or distance between two sequential scatterings) is much larger than the interaction range ($\sim 1/\mu$) of the potential in Eq. (1), the singularity in $A(\mathbf{q})$ can be neglected and the integration over ℓ_z (with respect to the $\hat{z}$ direction of $\mathbf{x}_{21} = \mathbf{x}_2 - \mathbf{x}_1 = L\hat{z} + \mathbf{r}_\perp$) gives us

$$\mathcal{M}^{(2)}_{\rm el} = 2\pi i\delta(E_i - E_f)\int\frac{d^2\ell_\perp}{(2\pi)^2}\bar{u}_{\sigma_f}(p_f)(-g^2)\Gamma_{(2)}u_{\sigma_i}(p_i),$$

$$\Gamma_{(2)} = \not{A}(\mathbf{p}_f-\mathbf{p})\frac{\not{p}}{2ip_z}\not{A}(\mathbf{p}-\mathbf{p}_i)e^{-i(\mathbf{p}-\mathbf{p}_i)\cdot\mathbf{x}_1 - i(\mathbf{p}_f-\mathbf{p})\cdot\mathbf{x}_2}, \tag{A5}$$

where $p = (E, \sqrt{E^2-\ell_\perp^2}, \ell_\perp)$ is the four-momentum of the internal line. One can derive the classical Glauber multiple collision cross section from this amplitude by averaging and summing over initial and final state ensemble of the target [10]. In the limit of high energy and small angle scattering, one can neglect the phase factor in the above equation and obtain the amplitude [as defined in Eq. (A1)]

$$f_2(E,t) = \frac{-i}{2\pi}\int d^2b\frac{1}{2!}[-\chi(\mathbf{b},E)]^2 e^{i\mathbf{q}_\perp\cdot\mathbf{b}}, \tag{A6}$$

where $1/2!$ comes from the different ordering of the target potentials and $\mathbf{q}_\perp = \mathbf{p}_{f\perp} - \mathbf{p}_{i\perp}$ is the total transverse momentum transfer due to the multiple scatterings. The eikonal function $\chi_{\sigma_1,\sigma_2}(\mathbf{b},E)$ is defined as the Fourier transform of the single scattering amplitude (in addition a factor $i/2\pi$):

$$\chi_{\sigma_2,\sigma_1}(\mathbf{b},E) \equiv -\int\frac{d^2q_\perp}{(2\pi)^2}e^{-i\mathbf{q}_\perp\cdot\mathbf{b}}\frac{g}{2Ei}\bar{u}_{\sigma_2}(p_2) \times\not{A}(\mathbf{q}_\perp)u_{\sigma_1}(p_1). \tag{A7}$$

In the definition of the product of eikonal functions, summation over the polarizations of the intermediate lines is implied:

$$\chi^n \equiv \sum_{\sigma_1,\ldots,\sigma_{n-1}}\chi_{\sigma_f,\sigma_{n-1}}\chi_{\sigma_{n-1},\sigma_{n-2}}\cdots\chi_{\sigma_1,\sigma_i}. \tag{A8}$$

One can generalize the double scattering amplitude to multiple scatterings and sum them together to get the total amplitude:

$$f(E,t) = \sum_{n=1}^{\infty}f_n(E,t) = \frac{-i}{2\pi}\int d^2b\frac{1}{n!}[-\chi(\mathbf{b},E)]^n e^{i\mathbf{q}_\perp\cdot\mathbf{b}} = \frac{i}{2\pi}\int d^2b[1-e^{-\chi(\mathbf{b},E)}]e^{i\mathbf{q}_\perp\cdot\mathbf{b}}. \tag{A9}$$

This is recognized as the elastic amplitude in the eikonal formalism. One can generalize this to the case of Pomeron exchange so that one can obtain both the total and inelastic cross sections for hadron-hadron collisions [29,30].

For radiation induced by double scatterings, there are contributions from three different diagrams as illustrated in Fig. 2. The total amplitude can be written as

$$\mathcal{M}^{(2)}_{\rm rad} = 2\pi i\delta(E_i - E_f - \omega)\int\frac{d^2\ell_\perp}{(2\pi)^2}\bar{u}(p_f)(-g^3) \times[\Gamma_a + \Gamma_b + \Gamma_c]u(p_i), \tag{A10}$$

$$\Gamma_a = \int \frac{d\ell_z}{2\pi} \not{A}(\mathbf{p}_f - \ell) \left[\frac{\not{\ell}}{\ell^2 + i\epsilon}\right]_{\ell^0 = E} \times \not{A}(\ell + \mathbf{k} - \mathbf{p}_i) \frac{\not{p}_i - \not{k}}{(p_i - k)^2} \not{\varepsilon} \times e^{-i(\ell + \mathbf{k} - \mathbf{p}_i)\cdot \mathbf{x}_1 - i(\mathbf{p}_f - \ell)\cdot \mathbf{x}_2}, \quad \text{(A11)}$$

$$\Gamma_b = \int \frac{d\ell_z}{2\pi} \not{A}(\mathbf{p}_f + \mathbf{k} - \ell) \times \left[\frac{\not{\ell} - \not{k}}{(\ell - k)^2 + i\epsilon} \not{\varepsilon} \frac{\not{\ell}}{\ell^2 + i\epsilon}\right]_{\ell^0 = E + \omega} \times \not{A}(\ell - \mathbf{p}_i) e^{-i(\ell - \mathbf{p}_i)\cdot \mathbf{x}_1 - i(\mathbf{p}_f + \mathbf{k} - \ell)\cdot \mathbf{x}_2}, \quad \text{(A12)}$$

$$\Gamma_c = \int \frac{d\ell_z}{2\pi} \not{\varepsilon} \frac{\not{p}_f + \not{k}}{(p_i + k)^2} \not{A}(\mathbf{p}_f + \mathbf{k} - \ell) \left[\frac{\not{\ell}}{\ell^2 + i\epsilon}\right]_{\ell^0 = E + \omega} \times \not{A}(\ell - \mathbf{p}_i) e^{-i(\ell - \mathbf{p}_i)\cdot \mathbf{x}_1 - i(\mathbf{p}_f + \mathbf{k} - \ell)\cdot \mathbf{x}_2}, \quad \text{(A13)}$$

where we have denoted $E = E_f = E_i - \omega$. Similarly as in double elastic scattering, one can integrate over ℓ_z and obtain

$$\Gamma_a = \not{A}(\mathbf{p}_f - \mathbf{p}) \frac{\not{p}}{2ip_z} \not{A}(\mathbf{p} + \mathbf{k} - \mathbf{p}_i) \left(-\frac{\varepsilon \cdot p_i}{k \cdot p_i}\right) \times e^{-i(\mathbf{p} + \mathbf{k} - \mathbf{p}_i)\cdot \mathbf{x}_1 - i(\mathbf{p}_f - \mathbf{p})\cdot \mathbf{x}_2}, \quad \text{(A14)}$$

$$\Gamma_c = \not{A}(\mathbf{p}_f + \mathbf{k} - \mathbf{p}') \frac{\not{p}'}{2ip'_z} \not{A}(\mathbf{p}' - \mathbf{p}_i) \left(\frac{\varepsilon \cdot p_f}{k \cdot p_f}\right) \times e^{-i(\mathbf{p}' - \mathbf{p}_i)\cdot \mathbf{x}_1 - i(\mathbf{p}_f + \mathbf{k} - \mathbf{p}')\cdot \mathbf{x}_2}, \quad \text{(A15)}$$

where we have used Dirac equations for the spinors and taken the soft radiation limit (neglecting terms like $\not{\varepsilon}\not{k}$). Notice that the four-momenta for the intermediate line between two scatterings before and after the radiation are different:

$$p = (E, \sqrt{E^2 - \ell_\perp^2}, \ell_\perp), \quad p' = (E + \omega, \sqrt{(E + \omega)^2 - \ell_\perp^2}, \ell_\perp). \quad \text{(A16)}$$

Define $\phi_D = -(\mathbf{p} - \mathbf{p}_i)\cdot \mathbf{x}_1 - i(\mathbf{p}_f - \mathbf{p})\cdot \mathbf{x}_2 = p_z L + \ell_\perp \cdot \mathbf{r}_\perp + \mathbf{p}_i \cdot \mathbf{x}_1 - \mathbf{p}_f \cdot \mathbf{x}_2$ as the phase factor for double elastic scattering, the corresponding phase factors in the above two amplitudes for induced radiation become

$$\phi_a = \phi_D + ik \cdot x_1, \quad \phi_c = \phi_D + ik \cdot x_2, \quad \text{(A17)}$$

where we used $p'_z \simeq p_z + \omega/v_z$, $v_z = p_z/E$ and we defined the time components of the four-coordinates as $t_1 = 0$, $t_2 = L/v_z$. These two terms can be identified with the initial radiation of the first scattering and the final state radiation of the second scattering, respectively.

In the amplitude of the radiation from the middle line, Γ_b, we can see that there are singularities in both of the two propagators. They should both contribute to the integration over ℓ_z. To complete the integration, we may use the identity (with $k^2 = 0$)

$$[(\ell - k)^2 + i\epsilon]^{-1}[\ell^2 + i\epsilon]^{-1} = \frac{[(\ell - k)^2 + i\epsilon]^{-1}}{2k \cdot (\ell - k)} - \frac{[\ell^2 + i\epsilon]^{-1}}{2\ell \cdot k}. \quad \text{(A18)}$$

With $\ell^0 = E + \omega$, the singularity in the second term put the internal line before the radiation vertex on mass shell with four-momentum p'. This contribution corresponds to the initial state radiation of the second scattering. For the first term in the above equation, we can make a variable change $\ell' = \ell - k$. With $\ell'_0 = E$, the internal line after the radiation vertex is put on shell with four-momentum p. This term can be identified as the final state radiation of the first scattering. Using identities

$$\not{p} \not{\varepsilon} (\not{p} + \not{k}) = 2\varepsilon \cdot p \not{p}, \quad \text{(A19)}$$

$$(\not{p}' - \not{k}) \not{\varepsilon} \not{p}' = 2\varepsilon \cdot p' \not{p}', \quad \text{(A20)}$$

one has the amplitude of the radiation from the middle line between two scatterings:

$$\Gamma_b = \not{A}(\mathbf{p}_f - \mathbf{p}) \frac{\not{p}}{2ip_z} \not{A}(\mathbf{p} + \mathbf{k} - \mathbf{p}_i) \left(\frac{\varepsilon \cdot p}{k \cdot p}\right) e^{i\phi_D + ik\cdot x_1} + \not{A}(\mathbf{p}_f + \mathbf{k} - \mathbf{p}') \frac{\not{p}'}{2ip'_z} \not{A}(\mathbf{p}' - \mathbf{p}_i) \left(-\frac{\varepsilon \cdot p'}{k \cdot p'}\right) \times e^{i\phi_D + ik\cdot x_2}. \quad \text{(A21)}$$

Summing all contributions together, we have the total amplitude for radiation induced by double scatterings:

$$\Gamma_a + \Gamma_b + \Gamma_c = -\not{A}(\mathbf{p}_f - \mathbf{p}) \frac{\not{p}}{2ip_z} \not{A}(\mathbf{p} + \mathbf{k} - \mathbf{p}_i) \times \left(\frac{\varepsilon \cdot p_i}{k \cdot p_i} - \frac{\varepsilon \cdot p}{k \cdot p}\right) e^{i\phi_D + ik\cdot x_1} - \not{A}(\mathbf{p}_f + \mathbf{k} - \mathbf{p}') \frac{\not{p}'}{2ip'_z} \not{A}(\mathbf{p}' - \mathbf{p}_i) \times \left(\frac{\varepsilon \cdot p'}{k \cdot p'} - \frac{\varepsilon \cdot p_f}{k \cdot p_f}\right) e^{i\phi_D + ik\cdot x_2}, \quad \text{(A22)}$$

which has two distinct contributions induced by each scattering. In the high-energy and small-angle scattering limit, we can neglect the small momentum transfer at each scattering as compared to the beam energy E. We also assume the soft radiation limit in which $k_\perp \ll q_\perp$, with $q_\perp$ being the transverse momentum transfer at each elastic scattering. Substituting the above expression back into Eq. (A10), the total amplitude factorizes as

$$\mathcal{M}^{(2)}_{\text{rad}} \approx \mathcal{M}^{(2)}_{\text{el}} i\mathcal{R}^{\text{QED}}_2, \quad \text{(A23)}$$

with the double elastic amplitude $\mathcal{M}^{(2)}_{\text{el}}$ given by Eq. (A5) and the radiation amplitude $\mathcal{R}^{\text{QED}}_2$ by Eq. (21).

In the case of gluon radiation in QCD, we will have different color matrices for different diagrams in Fig. 2. With the color indices as defined in Fig. 2, the corresponding color factors for Γ_a, Γ_b, and Γ_c are, respectively,

$$\left(T^{a_2} T^{a_1} T^b\right)_{BB'} T^{a_1}_{A_1 A'_1} T^{a_2}_{A_2 A'_2}, \quad \left(T^{a_2} T^b T^{a_1}\right)_{BB'} T^{a_1}_{A_1 A'_1} T^{a_2}_{A_2 A'_2}, \quad \left(T^b T^{a_2} T^{a_1}\right)_{BB'} T^{a_1}_{A_1 A'_1} T^{a_2}_{A_2 A'_2}. \quad \text{(A24)}$$

When taking the high-energy limit, all the contributions have a common momentum dependence, $\epsilon \cdot p_i/k \cdot p_i \simeq \epsilon \cdot p/k \cdot p \simeq \epsilon \cdot p_f/k \cdot p_f \simeq 2\vec{\epsilon}_\perp \cdot \mathbf{k}_\perp/k_\perp^2$. One can immediately arrive at Eq. (23).

[1] H. H. Gutbrod, A. M. Poskanzer, and H. G. Ritter, Rep. Prog. Phys. **52**, 267 (1989).
[2] J. Barrette *et al.*, Phys. Rev. Lett. **73**, 2532 (1994).
[3] X.-N. Wang and M. Gyulassy, Phys. Rev. D **45**, 844 (1992).
[4] J. P. Blaizot and A. H. Mueller, Nucl. Phys. **B289**, 847 (1987).
[5] K. Kajantie, P. V. Landshoff, and J. Lindfors, Phys. Rev. Lett. **59**, 2527 (1987); K. J. Eskola, K. Kajantie, and J. Lindfors, Nucl. Phys. **B323**, 37 (1989).
[6] M. Gyulassy and M. Plümer, Phys. Lett. B **243**, 432 (1990).
[7] X.-N. Wang and M. Gyulassy, Phys. Rev. Lett. **68**, 1480 (1992).
[8] M. Gyulassy, M. Plümer, M. H. Thoma, and X.-N. Wang, in *Proceedings of the Fourth International Conference on Nucleus-Nucleus Collisions*, Kanazawa, Japan, 1991, edited by H. Toki *et al.* [Nucl. Phys. **A538**, 37c (1992)].
[9] T. S. Biró, B. Müller, and X.-N. Wang, Phys. Lett. B **283**, 171 (1992).
[10] M. Gyulassy and X.-N. Wang, Nucl. Phys. **B420**, 583 (1994).
[11] L. D. Landau and I. J. Pomeranchuk, Dokl. Akad. Nauk SSSR **92**, 92(1953); A. B. Migdal, Phys. Rev. **103**, 1811 (1956); E. L. Feinberg and I. J. Pomeranchuk, Suppl. Nuovo Cimento **3**, 652 (1956); Sov. Phys. JETP **23**, 132 (1966).
[12] A. I. Akhiezer and N. F. Shulga, Sov. Phys. Usp. **30**, 197 (1987).
[13] M. G. Ryskin, Sov. J. Nucl. Phys. **52**, 139 (1990).
[14] S. Gavin and J. Milana, Phys. Rev. Lett. **68**, 1834 (1992).
[15] A. H. Sorensen, Z. Phys. C **53**, 595 (1992).
[16] S. J. Brodsky and P. Hoyer, Phys. Lett. B **298**, 165 (1993).
[17] P. Jain and J. P. Ralston, Report No. Kansa 94-5-22 (unpublished).
[18] J. F. Gunion and G. Bertsch, Phys. Rev. D **25**, 746 (1982).
[19] Yu. L. Dokshitzer, V. A. Khoze, A. H. Mueller, and S. I. Troyan, Rev. Mod. Phys. **60**, 373 (1988).
[20] B. Andersson, G. Gustafson, G. Ingelman, and T. Sjöstrand, Phys. Rep. **97**, 31 (1983); B. Andersson, G. Gustafson, and T. Sjöstrand, Z. Phys. C **6**, 235 (1980).
[21] F. Niedermayer, Phys. Rev. D **34**, 3494 (1986).
[22] J. Cleymans, V. V. Goloviznin, and K. Redlich, Phys. Rev. D **47**, 173 (1993); **47**, 989 (1993).
[23] J. Knoll and R. Lenk, Nucl. Phys. **A561**, 501 (1993).
[24] A. Selikhov and M. Gyulassy, Phys. Lett. B **316**, 316 (1993); Phys. Rev. C **49**, 1726 (1994).
[25] J. D. Bjorken, Report No. Fermilab-Pub-82/59-THY, 1982 (unpublished); erratum (unpublished).
[26] M. H. Thoma and M. Gyulassy, Nucl. Phys. **B351**, 491 (1991).
[27] T. S. Biró, E. van Doorn, B. Müller, M. H. Thoma, and X.-N. Wang, Phys. Rev. C **48**, 1275 (1993).
[28] M. Gyulassy, M. Plümer, and X.-N. Wang, Report No. LBL-36736, 1995 (unpublished).
[29] X.-N. Wang, Phys. Rev. D **43**, 104 (1991).
[30] X.-N. Wang, Ph.D. thesis, University of Oregon, 1989.